Surface & Coatings Technology 205 (2010) S246–S251

Contents lists available at ScienceDirect

Surface & Coatings Technology

journal homepage: www.elsevier.com/locate/surfcoat

Effect of additive alloying element on plasma nitriding and carburizing behavior for austenitic stainless steels

Motoo Egawa [a,b,*], Nobuhiro Ueda [b], Kazuhiro Nakata [a], Masato Tsujikawa [c], Manabu Tanaka [a]

[a] Joining and Welding Research Institute, Osaka University, 11-1 Mihogaoka Ibaraki-shi, Osaka 567-0047, Japan
[b] Technology Research Institute of Osaka Prefecture, 2-7-1 Ayumino Izumi-shi, Osaka, Japan
[c] Department of Materials Science, Graduate School of Engineering, Osaka Prefecture University, 1-1 Gakuen-Cho Nakaku Sakai-shi, Osaka, Japan

ARTICLE INFO

Available online 3 August 2010

Keywords:
Plasma nitriding
Plasma carburizing
Austenitic stainless steel
S-phase
Additive alloying element

ABSTRACT

Austenitic stainless steels, well known for their good corrosion resistance, have not been used for industrial components exposed to severe friction because of low hardness and poor friction and wear properties. Low-temperature plasma nitriding or carburizing of austenitic stainless steels can produce a specific nitrided or carburized layer, so-called "S-phase", with high hardness and good corrosion resistance. In this study, various austenitic stainless steels were low-temperature plasma nitrided and carburized, and the effect of additive alloying elements on the S-phase characteristics was investigated by various analyzing techniques: observation using an optical microscope, transmission electron microscope, X-ray diffraction analysis, an anodic polarization measurement in 5% H_2SO_4 solution, and a friction and wear test using a ball-on-flat friction apparatus. The thickness of the nitrided and carburized layers increased with an increase in the process temperature, and the thickness of the layer formed on the AISI316 steel is thickest in all substrate steels. While, at above 'critical temperature' the corrosion resistances were deteriorated owing to the precipitation of chromium nitride or carbide. The critical temperature was dependent on the substrate material in nitriding. On the other hand, in the case of carburizing, the critical temperatures were almost constant with substrate materials. The corrosion resistances of the S-phase layers on most of the specimens were less than that of the untreated stainless steels, but the AISI316 and JIS-SUS304J3 steels carburized at 400 °C showed the same excellent corrosion resistances as the untreated steels respectively. The wear resistance of every stainless steel was obviously improved by nitriding or carburizing treatment.

1. Introduction

Austenitic stainless steels are widely used in many industrial parts owing to their excellent corrosion resistance. However, the use of austenitic stainless steels is not considered for parts exposed to severe friction because they have low hardness and poor friction and wear properties. Therefore, many attempts to harden the surface of these steels have been made. For example, a conventional nitriding treatment at 500–550 °C is well known to increase the surface hardness of the austenitic stainless steels and improve the wear resistance. However, hardening by the nitriding is induced by the precipitation of chromium nitrides in the nitrided layer. This leads to a depletion of chromium dissolved in the austenitic matrix and thus a significant reduction in corrosion resistance. Therefore, it is important to develop surface engineering techniques that can improve the wear resistance of austenitic stainless steels without the loss of corrosion resistance.

Low-temperature plasma nitriding can produce a new phase with high hardness and good corrosion resistance on austenitic stainless steel surfaces. It does so by the formation of a non-equilibrium supersaturated layer, what is called "S-phase" or "expanded austenite" [1,2]. This low-temperature diffusion processing is also effective for carburizing. Despite its very high nitrogen or carbon content, the S-phase has no chromium nitrides and carbides that consume the dissolved chromium in the austenitic matrix. Although much research [3–8] has been reported in the literature, the nature of the S-phase has not yet been fully characterized. Some papers have reported low-temperature nitriding for the commercial stainless steels of AISI 304, 316, 321, and 310 S [1–8]. But these papers are individually researched, there are few reports that report systematically on the effect of alloying elements.

The low-temperature plasma nitriding and carburizing characteristics of various austenitic stainless steels have been investigated in this work. The purpose of this paper is to discuss the response of various austenitic stainless steels to low-temperature plasma nitriding and carburizing, in terms of microstructures and properties.

* Corresponding author. Joining and Welding Research Institute, Osaka University, 11-1, Mihogaoka Ibaraki-shi, Osaka 567-0047, Japan. Tel.: +81 725 51 2694; fax: +81 725 51 2749.
E-mail address: egawa@tri.pref.osaka.jp (M. Egawa).

0257-8972/$ – see front matter © 2010 Elsevier B.V. All rights reserved.
doi:10.1016/j.surfcoat.2010.07.093

Table 1
Chemical composition of substrate materials (mass%).

	C	Si	Mn	P	S	Ni	Cr	Mo	Cu	Ti	Nb
AISI304	0.06	0.04	0.94	0.037	0.003	8.3	18.8	0.21	0.31	–	–
AISI316	0.04	0.70	0.94	0.030	0.003	10.2	17.0	2.34	0.24	–	–
JIS-SUS304J3	0.02	0.23	0.68	0.037	0.004	10.0	18.3	0.29	2.97	–	–
AISI321	0.03	0.46	1.04	0.019	0.001	9.5	17.9	0.17	0.17	0.32	0.00
AISI347	0.04	0.33	1.63	0.017	0.001	9.6	18.1	0.17	0.13	0.00	0.36

2. Experimental procedure

The substrate materials were commercial grade austenitic stainless steels AISI304, AISI316, JIS-SUS304J3 (a steel for which 1–3 wt.% copper has been added to AISI304), AISI321, and AISI347. The chemical compositions of the steels are listed in Table 1. Plasma nitriding or carburizing specimens were $50\times25\times5$mm in size and solution-treated at 1030 °C. The surfaces of the specimens were polished with emery papers and 3 μm diamond slurry. Plasma nitriding or carburizing was performed with a laboratory type apparatus with a conventional direct current (d.c.) power source. After the specimen was mounted on the cathode in a furnace, its vacuum bell jar was evacuated to 1.33×10^{-1} Pa. The specimens were plasma nitrided in a gas mixture of 80% nitrogen and 20% hydrogen for 4 h at various temperatures, and plasma carburized in a gas mixture of 50% argon, 45% hydrogen and 5% methane for 4 h. The pressures of the gas mixtures were adjusted to 667 Pa. Each specimen was mounted on the cathode and heated using glow discharge in the nitriding or carburizing processes without a pre-cleaning or pre-heating step. The temperature of the specimen was measured using a thermocouple. After the plasma treatment was finished, the specimen was allowed to cool in the evacuated furnace.

The treated specimens were then characterized by X-ray diffraction for phase identification using Cu-Kα radiation and a monochromator. Microstructures were observed using an optical microscope. Transmission electron microscopy (TEM) observation was carried out using HF-2000 (made by HITACHI High-Technologies Corp.) TEM specimens were prepared perpendicular to the surface. To examine the corrosion resistance of the specimen, anodic polarization characteristics in 5 mass% H_2SO_4 aq. solutions (about 0.51 mol/kg H_2SO_4 aq. solutions) were measured using a potentiostat. Friction and wear tests were carried out using a ball-on-flat friction apparatus to evaluate the tribological properties. The flat samples were slid in a reciprocating motion against balls 4.8 mm in diameter, made of three materials: bearing steel AISI 52100, AISI 304, and alumina. The average sliding speed was 20 mm/s, sliding stroke length was 5 mm, and sliding time was 2 h. All tests were run at room temperature in an open air at 50−60% relative humidity and under a 1.96 N load.

3. Results and discussion

Fig. 1 shows the cross-sectional microstructures of the nitrided layers in various stainless steels after plasma nitriding at various temperatures for 4 h. In the case of all stainless steels, at 400 °C, the nitrided layers appeared 'white' under an optical microscope, because the layers were resistant to the corrosive attack by the marble's reagent (mixture of equal parts of hydrochloric acid and $CuSO_4$ saturated aq. solution), and as nitriding temperatures increased, 'dark' phases appeared in the white layer. It can be shown that the formation

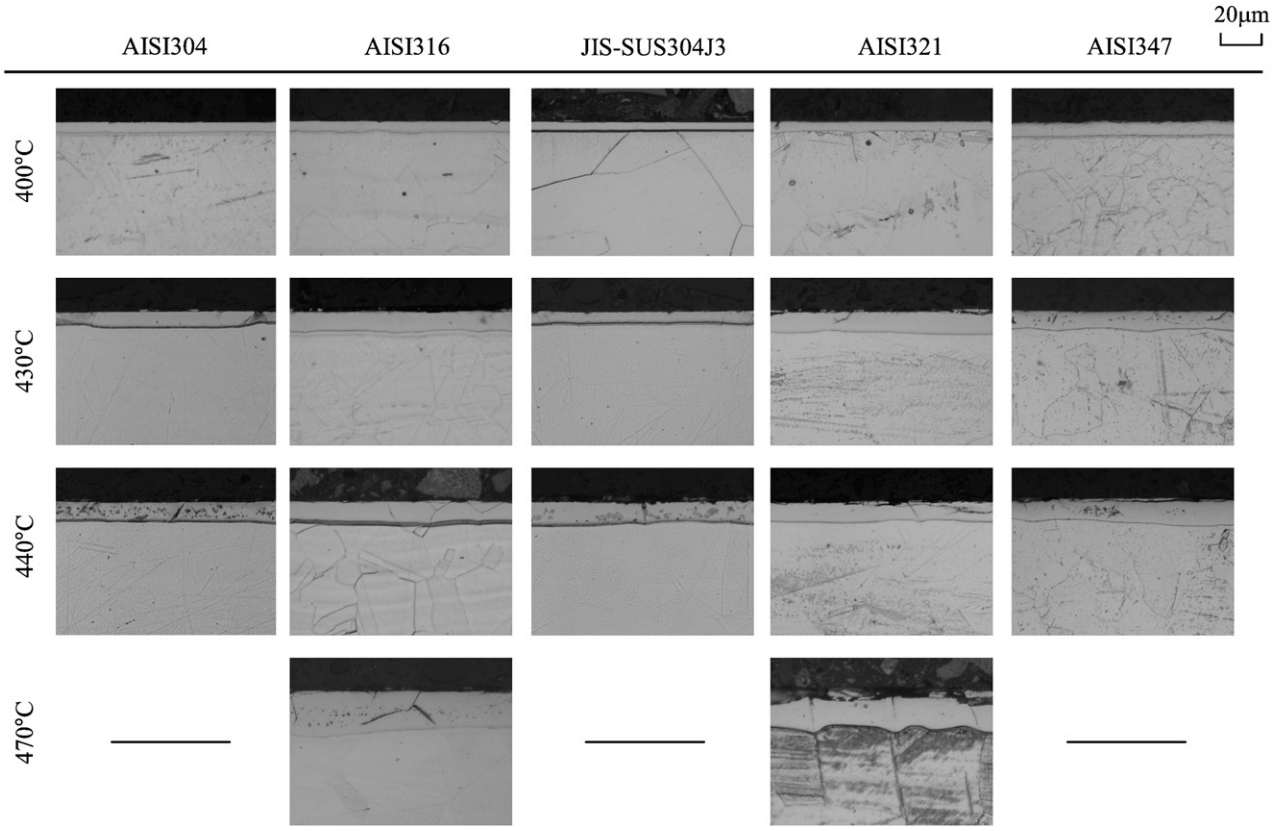

Fig. 1. Cross-sectional microstructures of the nitrided layers in various stainless steels after plasma nitriding at various temperatures for 4 h.

Table 2
Critical temperature to formation of precipitation; T1: at the grain boundary, T2: at the inter granular regions.

		304	316	304J3	321	347
Nitriding	T1 (°C)	430–440	430–440	430–440	430–440	430–440
	T2 (°C)	430–440	460–470	430–440	460–470	430–440

of these 'dark' phases is associated with the precipitation of chromium nitrides which thus deteriorates the corrosion resistance of the steel. Most of the dark phases were distributed uniformly in the nitrided layer, but some of them were along the grain boundaries. As can be seen in Fig. 1, there exist the critical temperatures for the formation of the 'dark' phases in the nitriding process. Thus, in order to obtain the layer with high hardness and high corrosion resistance, it is important to prevent the formation of the 'dark' phases by using a sufficiently low temperature. In addition, the critical temperatures are different for the stainless steel grades. Table 2 summarizes the T1 and T2 values, where T1 is the critical temperature where the 'dark' phase appears along the grain boundary and T2 is the temperature where they appear at the intragranular region. From Table 2, it can be seen that the critical temperature T1 is almost constant with the substrate material. On the other hand, T2 is dependent on the substrate materials; the T2 of AISI316 and AISI321 are higher than that of other materials. This reflects the influence of the substrate chemical composition on the stability of low-temperature nitrided layers. That is, molybdenum in 316 steel and titanium in 321 steel stabilize the structure of the S-phase by preventing the precipitation of chromium nitrides by attracting nitrogen atoms around themselves. However, copper in JIS-SUS304J3 did not affect on the stability of the S-phase, because they have no tendency to attract nitrogen atoms in steel, therefore they did not affect to the formation of the nitride

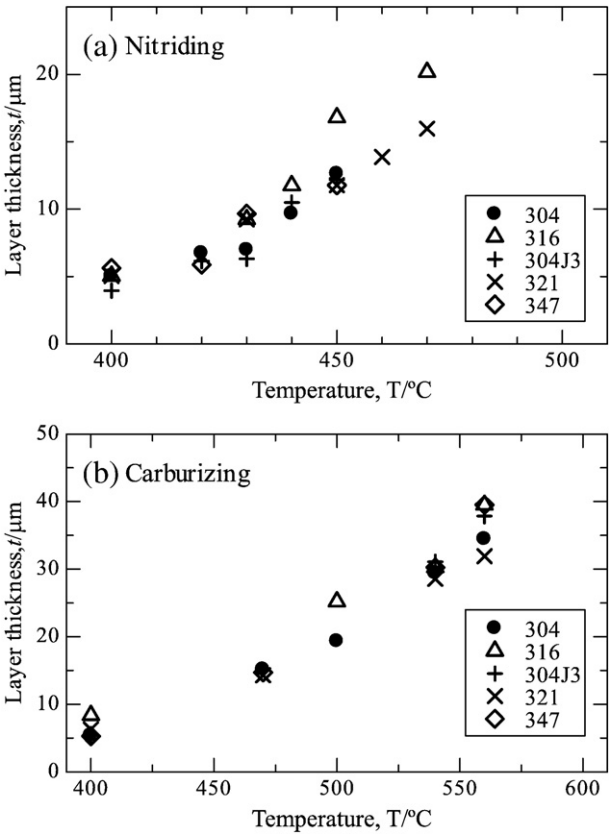

Fig. 3. The relationships between layer thickness and processing temperature in (a) nitriding, and (b) carburizing.

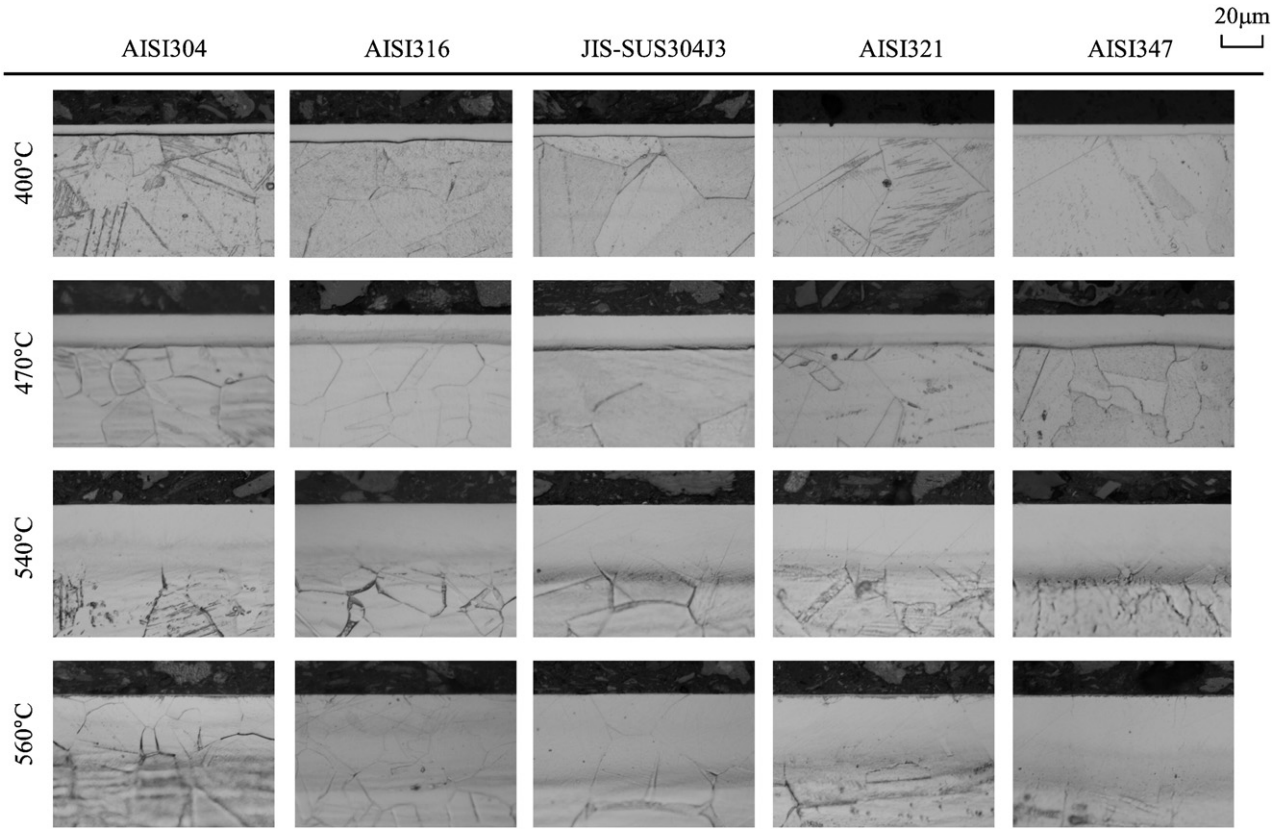

Fig. 2. Cross-sectional microstructures of the carburized layers in various stainless steels after plasma carburizing at various temperatures for 4 h.

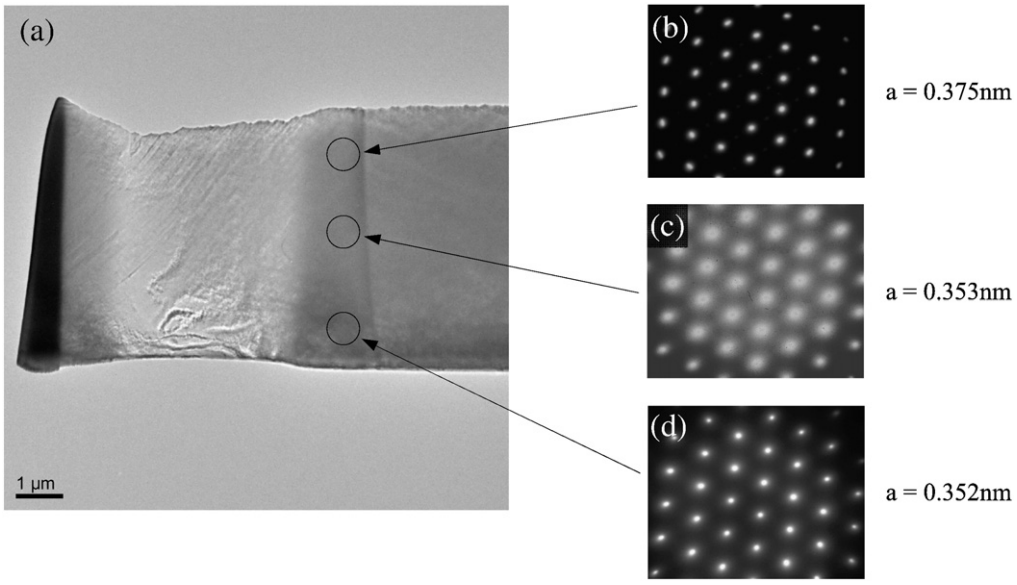

Fig. 4. (a) TEM image and ((b)–(d)) the corresponding selected area diffraction (SAD) patterns for the layers of the nitrided at 400 °C on AISI304.

precipitation. Although niobium in AISI347 has a tendency to attract nitrogen atoms, the critical temperature T2 of AISI347 was equal to that of AISI304. The reason why niobium could not act on preventing the precipitation of chromium nitrides seems that most of niobium were combined with carbon in the steel. On the other hand, the grain boundary which is the priority site for the precipitation of chromium nitrides was not affected by the alloying element, because at that site there are easy to precipitate chromium nitrides.

Fig. 2 shows the cross-sectional microstructures of the carburized layers in various steels after plasma carburizing at various temperatures for 4 h. In the case of all stainless steels, at the temperatures below 540 °C, the surface layers appeared 'whitish'. Although, at 560 °C, the outmost edges of the surface layers exhibit 'dark' appearance, and the grain boundaries in the nitrided layer were also etched by the reagent. In the case of carburizing, the critical temperatures to form the 'dark' phase were from 540 to 560 °C, which were almost constant with steel grades.

As can be seen in Figs. 1 and 2, the thickness of the layers increased with an increase in the processing temperature. The thicknesses of the layers against processing temperature on various stainless steels were shown in Fig. 3. In the case of plasma nitriding; Fig. 3(a), the relationship between the temperature and the thickness can be divided into two types; the former is the type where the layer grows slowly at low temperatures and then more rapidly above a critical temperature (in AISI 304, JIS-SUS304J3 and AISI347), and the latter is the type where the layer thicknesses show an approximately linear increase with an increase in the temperature (in AISI316 and AISI321). It seems that the precipitation of chromium nitrides brings about an acceleration of the growth of the overall nitrided layer in AISI304, JIS-SUS304J3 and AISI347. On the other hand, in the case of carburizing; Fig. 3(b), a distinct flexion point was not observed unlike in nitriding. In all substrate steels, the layer thicknesses increase with an increase in the temperature. Then, in general, it can be seen that the thickness of the layer formed on the AISI 316 steel is the thickest of all steels.

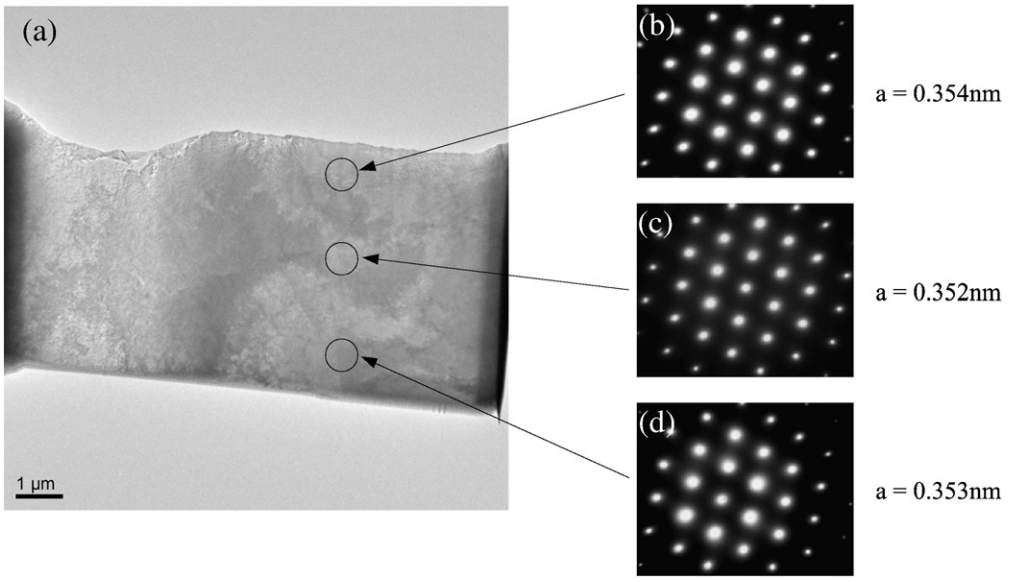

Fig. 5. (a) TEM image and ((b)–(d)) the corresponding selected area diffraction (SAD) patterns for the layers of the carburized at 450 °C on AISI304.

Figs. 4 and 5 show typical TEM images and the corresponding selected area diffraction (SAD) patterns from nitrided and carburized layers in AISI304. Both TEM specimens were cut normal to the surface layer; each SAD pattern indicated by '(b)' was taken from near the top of the surface layer, and the SAD pattern indicated by '(d)' was taken from near the bottom of the surface layer. It can be seen that both layers have no precipitations and comprise a single phase which has a face centered cubic structure similar to that of the substrate austenite. The lattice parameters of the nitrided layers are larger than that of the substrate austenite: a = 0.348 nm. In addition, the top of the nitrided layer (Fig. 4(b)) has a larger lattice parameter than the bottom of the nitrided layer (Fig. 4(d)). On the other hand, in the case of the carburized specimen, the lattice parameters in the layer are almost equal without regard to the depth from the surface.

Fig. 6 shows typical anodic polarization curves in 5 mass% H_2SO_4 aq. solution for AISI316 steels in nitriding at 400 °C, carburizing at 400 °C, and the untreated specimen. In the H_2SO_4 solution, the current density to maintain passivity on the nitrided AISI316 is higher than that of the untreated specimen. On the other hand, that on the carburized specimen is almost same as that on the untreated specimen. The comparable result was observed in JIS-SUS304J3. Though, in the case of other steels, the corrosion resistances of the nitrided and carburized specimens were slightly deteriorated compared with the untreated specimens.

Fig. 7 shows the variation of friction coefficients of the 304 J3 steels nitrided at 400 °C and the untreated specimens slide against various balls. Against AISI 304 and AISI 52100 balls, the friction coefficients of the nitrided specimens are almost the same as those of the untreated specimens. On the other hand, against an alumina ball, the nitrided specimen had a friction coefficient of about 0.55, while an untreated specimen had a coefficient of about 0.7.

Fig. 8 shows the wear volume on the specimen after sliding. The wear volumes were calculated from the shape of the wear tracks. Against the balls of all materials, especially against the ball of an alumina, the wear volumes of the nitrided specimens were less than one tenth of those of the untreated specimens. Above all, plasma treated specimens show excellent wear resistance compared with the untreated specimens.

4. Conclusions

In this study, various austenitic stainless steels were low-temperature plasma nitrided and carburized, and the effect of additive alloying elements on the S-phase characteristics was investigated. The thickness of the nitrided and carburized layers increased with an increase in the process temperature, and the thickness of the layer formed on the AISI316 steel is the thickest of all substrate steels. While, at above 'critical temperature', the corrosion resistance was

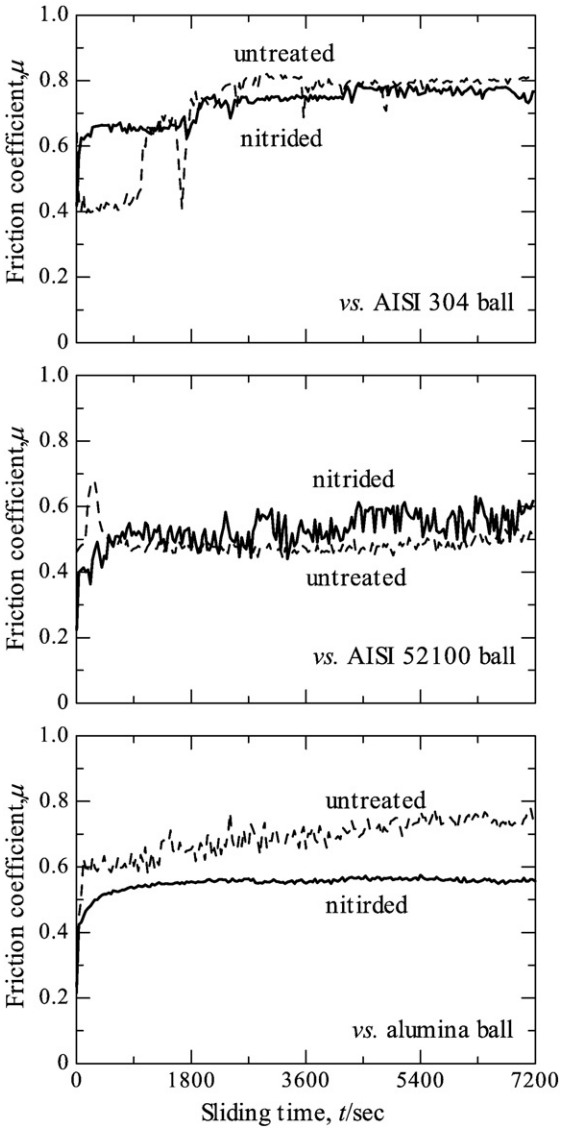

Fig. 7. Variations of the friction coefficient of JIS-SUS304J3 (a) untreated and (b) nitrided at 400 °C against various balls.

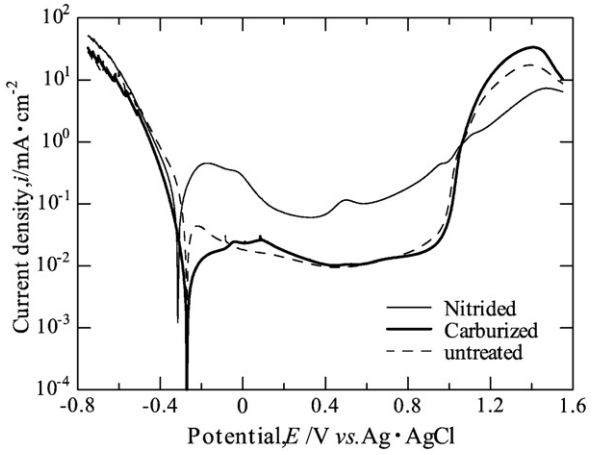

Fig. 6. Anodic polarization curves for the AISI316 steel in 5% H_2SO_4 aq. solution.

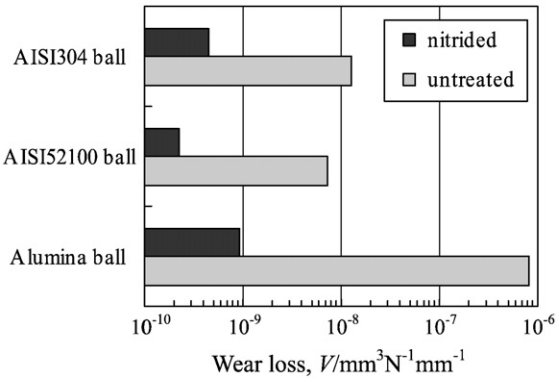

Fig. 8. Wear loss of untreated and nitrided JIS-SUS304J3 against various balls.

deteriorated owing to the precipitation of chromium nitrides or carbides. In nitriding, the critical temperatures depend on the stainless steel grades. On the other hand, in the case of carburizing, the critical temperatures were almost constant with the stainless steel grades. The corrosion resistances of the S-phase layers on most of all specimens were less than that of the untreated stainless steels, but the AISI316 and JIS-SUS304J3 steels carburized at 400 °C showed the same excellent corrosion resistances as the untreated steels respectively. The wear resistance of every stainless steel was obviously improved by nitriding or carburizing treatment.

References

[1] K. Ichii, K. Fujimura, T. Takase, Technol. Rep. Kansai Univ. 27 (1986) 135.
[2] M.J. Baldwin, M.P. Fewell, S.C. Haydon, S. Kumar, G.A. Collins, K.T. Short, J. Tendys, Surf. Coat. Technol. 98 (1998) 1187.
[3] Z.L. Zhang, T. Bell, Surf. Eng. 1 (1985) 131.
[4] Y. Sun, T. Bell, Z. Kolosvary, J. Flis, Heat Treat. Met. 1 (1999) 9.
[5] M.P. Fewell, D.R.G. Mitchell, J.M. Priest, K.T. Short, G.A. Collins, Surf. Coat. Technol. 131 (2000) 300.
[6] T. Christiansen, M.A.J. Somers, Scr. Mater. 50 (2004) 35.
[7] M. Tsujikawa, N. Yamauchi, N. Ueda, T. Sone, Y. Hirose, Surf. Coat. Technol. 193 (2005) 309.
[8] E. Menthe, K.-T. Rie, J.W. Schultze, S. Simson, Surf. Coat. Technol. 74–75 (1995) 412.